Computers and Electronics in Agriculture 193 (2022) 106601

Contents lists available at ScienceDirect

Computers and Electronics in Agriculture

journal homepage: www.elsevier.com/locate/compag

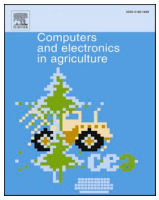

Original papers

A novel method of fish tail fin removal for mass estimation using computer vision

Yinfeng Hao [a,b], Hongjian Yin [c], Daoliang Li [a,b,*]

[a] College of Information and Electrical Engineering, China Agricultural University, Beijing 100083, China
[b] National Innovation Center for Digital Fishery, China Agricultural University, Beijing 100083, China
[c] College of Computer and Communication Engineering, University of Science and Technology Beijing, Beijing 100083 China

ARTICLE INFO

Keywords:
Tail fin removal
Automation
Fish
Mass estimation
Computer vision

ABSTRACT

Fish mass estimation is extremely important for farmers to get fish biomass information, which could be useful to optimize daily feeding and control stocking densities and ultimately determine optimal harvest time. However, fish tail fin mass does not contribute much to total body mass. Additionally, the tail fin of free-swimming fish is deformed or bent for most of the time, resulting in feature measurement errors and further affecting mass prediction accuracy by computer vision. To solve this problem, a novel non-supervised method for fish tail fin removal was proposed to further develop mass prediction models based on ventral geometrical features without tail fin. Firstly, fish tail fin was fully automatically removed using the Cartesian coordinate system and image processing. Secondly, the different features were respectively extracted from fish image with and without tail fin. Finally, the correlational relationship between fish mass and features was estimated by the Partial Least Square (PLS). In this paper, tail fins were completely automatically removed and mass estimation model based on area and area square has been the best tested on the test dataset with a high coefficient of determination (R^2) of 0.991, the root mean square error (RMSE) of 7.10 g, the mean absolute error (MAE) of 5.36 g and the maximum relative error (MaxRE) of 8.46%. These findings indicated that mass prediction model without fish tail fin can more accurately estimate fish mass than the model with tail fin, which might be extended to estimate biomass of free-swimming fish underwater in aquaculture.

1. Introduction

Aquatic products as a vital source of nutritious protein, make up of human diet all around the world (FAO, 2020). Recently, fish farming has been developed rapidly in food production. And fish mass estimation is beneficial to obtain biomass information in aquaculture, which has played a critical role in optimizing feed regimens to avoid under- or overfeeding, controlling oxygen consumption and antibiotic dose, and determining optimal harvest time for aquaculture managers (Lines et al., 2001). In addition, accurate size measurements can be used to keep homogenous size batches in intensive fish farming, which is beneficial to fish welfare by reducing their aggression (Ashley, 2007).

The conventional method to gain the information on fish mass is by periodic sampling and weighing (Saberioon and Cisar, 2018). Normally, the average weight of samples is estimated by collecting a given number of fish from ponds or cages. However, the manual sampling is usually time-consuming, labor-intensive, expensive and has an inherent error of 15–25% (Klontz and Kaiser, 1993). Furthermore, manual sampling can also bring great stress to fish, affecting their growth and even resulting in the death (Li et al., 2020). Therefore, it is very urgent to automatically measure fish mass without manual handling, which is of great interest for aquaculture administrators.

With the development of new information technologies, the non-invasive computer vision techniques have been attracting interest of researchers and practitioners in aquaculture communities during the past three decades (Costa et al., 2009; Saberioon et al., 2017; Zhou et al., 2018; Zhou et al., 2019a; Zhou et al., 2019b; Zion, 2012). Fish size such as length, area and height is a vitally important parameter at different growth stages (Shi et al., 2020). The computer vision provides an automatic and effective means for remotely estimating fish size (Garcia et al., 2020; Monkman et al., 2020; Munoz-Benavent et al., 2018b; Puig-Pons et al., 2019), which makes it possible to measure fish biomass using fish size-weight relations. To the best of our knowledge, there is no a general model for mass estimation of each species, the optimal model

* Corresponding author at: P. O. Box 121, China Agricultural University, 17 Tsinghua East Road, Beijing 100083, China.
E-mail address: dliangl@cau.edu.cn (D. Li).

https://doi.org/10.1016/j.compag.2021.106601
Received 12 April 2021; Received in revised form 22 November 2021; Accepted 27 November 2021
Available online 3 January 2022

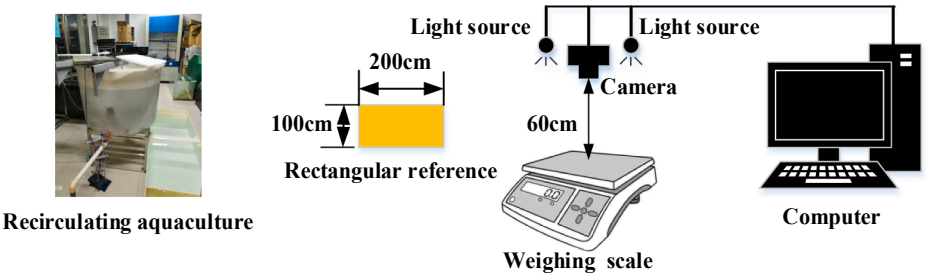

Fig. 1. The experimental equipment system.

needs to be developed for each species individually. Beddow et al. (1996) adopted stereo camera systems to predict the weight of Atlantic salmon (*Salmon salar L.*) based on multi-parameters extracted from images with an error of (−0.1 ± 9.0) %. Odone et al. (2001) used computer vision systems based on different subsets of 13 shapes available from top and side views to predict fish weight by Support Vector Machine. Dios et al. (2003) also adopted stereovision system to estimate fish mass by simple length-weight relations well known in aquaculture domain. Costa et al. (2013) developed the model based on external shape from fish lateral images to estimate weight of cultured sea bass (*Dicentrarchus labrax*). In addition, Saberioon and Cisar (2018) used RGB-D camera to estimate fish mass based on eight dorsal geometrical features and machine learning algorithms with the highest R^2 of 0.872. Zhang et al. (2020) proposed principal component analysis–calibration factor and neural network to estimate fish mass from images with the mean absolute error of 0.0104, the root mean square error of 0.0137 and the coefficient of determination of 0.9021. Besides, Al-Jubouri et al. (2017) designed a dual synchronized orthogonal webcams system to estimate zebrafish length with average error approximately 1% and Rizzo et al. (2017) showed paired-laser photogrammetric approach to measure length of small benthic free-swimming fish and the magnitude of differences was ranging from 0.6% to 3.1% between direct and photogrammetric measurements. Manuel Miranda and Romero (2017) proposed a third-order regression curve approximated rainbow trout (*Oncorhynchus mykiss*) silhouette to estimate length of free-swimming fish by computer vision.

However, the caudal fin of free-swimming fish underwater is deformed or bent for most of the time, which causes errors in size measurement using computer vision, further resulting in mass measurement errors. In addition, the fish fin mass does not contribute much to total body mass (Balaban et al., 2010b). For possibly better accuracy of mass measurement, it is necessary to remove tail fin from fish image to extract shape features for establishing mass model, so that the model can help to better predict biomass of free-swimming fish in water. The earliest study proposed by Balaban et al. (2010a) showed that the R^2 values of the power equation based on view area to predict weight of fish with and without tail fins are the same: 0.993. Subsequently, de Verdal et al. (2014) performed several measurements on digital pictures of sea bass larvae to estimate body weight. In this study, the mass model based on five features without considering tail fin had higher correlation coefficient than in Costa et al. (2013). The reason may be that image processing excluded the transparent fin, which the weight is negligible. Subsequently, Viazzi et al. (2015) indicated that model based on area from fish side view without considering tail fin performed well to predict Jade perch (Scortum barcoo) mass with the R^2 of 0.99. However, the proposed method of tail fin removal is not fully automated and requires manual intervention. Munoz-Benavent et al. (2018a) presented the deformable model at five predefined silhouette points of ventral silhouette proposed by Atienza-Vanacloig et al. (2016) to estimate length of bluefin tuna (Thunnus Thynnus) using stereovision system. The caudal fin contour was not modeled because its shape varies widely. In addition, Konovalov et al. (2019) showed the no-fins based Convolutional Neural Network (CNN) performed best to estimate Nile tilapia weight on test images with the MAPE of 4.28%. Fernandes et al. (2020) used the CNN for automatic segmentation of Nile tilapia and the no fish tin segmentations obtained from the best network were used to extract area, length, height. The predictive model included area and its square as predictor variables achieved R^2 of 0.96. Although the CNN can be used to remove fish fin, it is supervised learning, which requires a large number of samples to be manually marked for training and different markers from different person could introduce errors. Since the fins removal would require extra work and computing time, there are limited literatures about the tail fin removal from fish images. Therefore, it is very urgent to develop an effective and automatic non-supervised method for tail fin removal on fish mass measurement.

The aim of this study was to develop a new fully automatic method to remove the tail fin from fish image, which was useful to establish the more accurate model of mass prediction using computer vision. The specific objectives of this study were to (1) fully automatically remove fish tail fin based on Cartesian coordinate system and image processing, (2) respectively extract the different features from fish image with and without tail fin, (3) develop mass prediction model based on ventral geometrical features with and without tail fin, (4) verify the precision of the proposed method for mass estimation in validation set.

2. Materials and methods

2.1. Animals and housing

The experiment was carried out in the B17 lab at National Innovation Center for Digital Fishery, China Agricultural University, China. During the experiment, 80 crucian carp (*Carassius auratus gibelio*) in different sizes were purchased from aquatic farm in suburban areas of Beijing. And then, they were farmed for near four months in a recirculating aquaculture system which consisted of 3 tanks. Each tank has a capacity of 600L and equipped with an external mechanical filter and four built-in filters, a nitrifying trickling filter to maintain NH3-N and NO2-N levels, a water pump to regularly replace half the water in the tank with new water during fish farming, an oxygen reactor, a pH pump, two heating rods (Elecro 500 w, Sunsun) and a denitrifier to maintain NO3-N levels. The oxygen, temperature and pH were monitored continuously and were kept between 7.0–8.5 mg/l, 24 ± 3 ∘C and 7.5–8.5, respectively.

2.2. Data collection

Fish were netted and mildly anesthetized with tricaine methane sulfonate (MS-222) in a water basin before data acquisition so as to minimize stress. Each fish was caught to be weighed for three replicates and then individually pictured. Three replicates were made for comparing with those estimated by non-contact method. In farming process, fish was pictured and weighed in five measurement sessions with an interval of approximately 25 days, and the number of fish left in each session is 80, 68, 60, 55, 52 respectively because of fish death, adding up to a total 315 fish. Using sterile paper to wipe the water off fish before weighing, these fishes were weighed manually by using

Table 1
The relevant description and definition of each feature.

Feature	The definition of features
Area (A_1, A_2)	Number of pixels in fish binary image region with and without tail fin
Length (L_1)	The total length of the fish
Height (H_1)	The height of minimum bounding rectangle
Height (H_2)	The fish width passing through centroid coordinate
Height (T_2)	The fish width passing through the middle point between centroid coordinate and tail handle
Height (S_2)	The width is symmetric with T_2 respect to centroid coordinate
Length (L_2)	The length between fish snout and tail handle

weighing scale (YHC-L01) with a precision of 0.1 g. Then, each fish was pictured from a distance of 60 cm using MV-EM510M CCD camera (Microvision, China) with a focal length of 6 mm, exposure of 12.5 ms, ISO of 200 and resolution of 2456 × 2058 pixels. Simultaneously, the background without fish were also pictured to be used for subsequent background subtraction. The image had three components (red, green and blue) with each color comprising 256 graduations. The experimental equipment is illustrated in Fig. 1.

A total 315 fish images were collected indoors under artificial lighting with the 315 fish images * 3 measurements of mass. The average mass for each crucian was obtained after 3 replicate measurements. The minimum measured mass of fish was 68.1 g, while the maximum measured mass was 298.4 g. The setup was remounted at the beginning of every measurement session. A was fish body surface area in cm^2 (with or without fins), L was fish length in cm (with or without fins) and H was fish height in cm (with or without fins). In order to compensate small variations in setup of different measurement sessions, the rectangular reference (200 mm × 100 mm) that placed in center of tray is pictured each time for conversion of pixel measures to millimeters. And the area, length and height of the bounding-box surrounding the rectangular reference were then used to rescale fish size.

2.3. Image analysis

The image analysis which includes five steps namely a) Pre-processing, b) Segmentation, c) Removing the tail fin, d) Feature extraction, as shown in Table 1, and e) Regression algorithm, have been developed in MatlabR2014a (MathWorks, MA, USA) environment. Fig. 2 shows the main procedures of image analysis.

2.3.1. Pre-processing

The image is too large, so it has to be reduced for image analysis. In addition, image quality might be affected by many factors such as noise during fish image acquisition. In our case, the image difference method proposed by Siewert et al. (2014) that can determine the rough position of the target is adapted to remove the influence of uneven environmental illumination. Additionally, the linear transformation proposed by Gonzalez et al. (2018) was used to increase the contrast of difference images to clarify the boundaries of the whole fish. And the linear transformation can be expressed as:

$$I = F_a{}^*C + \frac{F_b}{255} \tag{1}$$

where the $F_a = 6$, $F_b = 55$ is obtained by trial and error. C is the differential image, I is the image obtained by the image pre-processing.

2.3.2. Segmentation

Image segmentation is a fundamental yet challenging task in image processing and computer vision, which denotes object separation from background. Active contour has been widely used for segmentation as it has the ability to find smooth and closed contour with sub-pixel accuracy (Kass et al. (1987)), which includes edge-based model and region-based model. In this study, the simplest and well-known region-based model which is active contour without edges proposed by Chan and Vese (2001) (C-V) was used for fish segmentation. And the algorithm is the minimization of energy for segmentation. The energy function can be written as

$$E(C) = \alpha^*L(C) + \beta^*Area(inside(C)) + E_{in}(C) + E_{out}(C) \tag{2}$$

where $L(C)$ is the length of the contour C, $Area(inside(C))$ is the area of the region inside C, $E_{in}(C) = \lambda_1 \int_{inside} |I(x,y) - c_1|dxdy$, $E_{out}(C) = \lambda_2 \int_{outside} |I(x,y) - c_2|dxdy$, $\alpha \geqslant 0$ and $\beta \geqslant 0$, c_1 and c_2 are the average gray value of inside and outside areas. $\alpha = 0.2, \beta = 0, \lambda_1 = \lambda_2 = 1$ are fixed parameters. From the above energy function, when the contour C is located in the border of two homogeneous area, $E(C)$ can achieve the minimum, and the global optimal segmentation is got. The specific calculation could be saw in reference (Chan and Vese, 2001). Here, a rectangular contour as the initial mask $m(0.3^*size(I,1) : 0.7^*size(I,1), 0.2^*size(I,2) : 0.8^*size(I,2))$ is established, where $size(I,1)$ and $size(I,2)$ are the total row and column numbers of image I pixels, respectively. The above method code is as follows: $Output = region\_seg(I, m, 500, 0.2)$. The output result is fish binary image F. However, a rectangular contour as the initial mask m and the evolution curve iterative times were not very well defined, this could cause error segmentation of images. In this study, according to this characteristic that the fish is roughly in the center of the image, the center pixel coordinate of image can be obtained. Hence, the row range of initial mask m is defined in the $0.2^*size(I,1)$ from the center of image I, that is $0.3^*size(I,1) : 0.7^*size(I,1)$. Similarly, the column range of initial mask m is defined in $0.3^*size(I,2)$

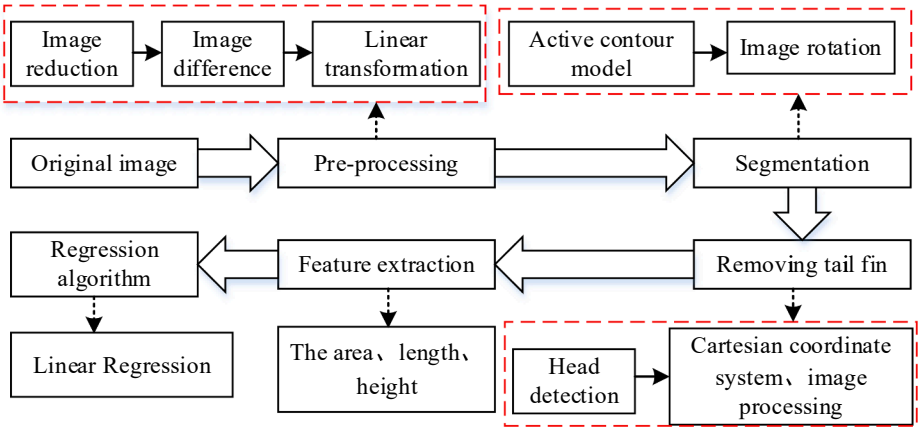

Fig. 2. The flowchart of the image analysis.

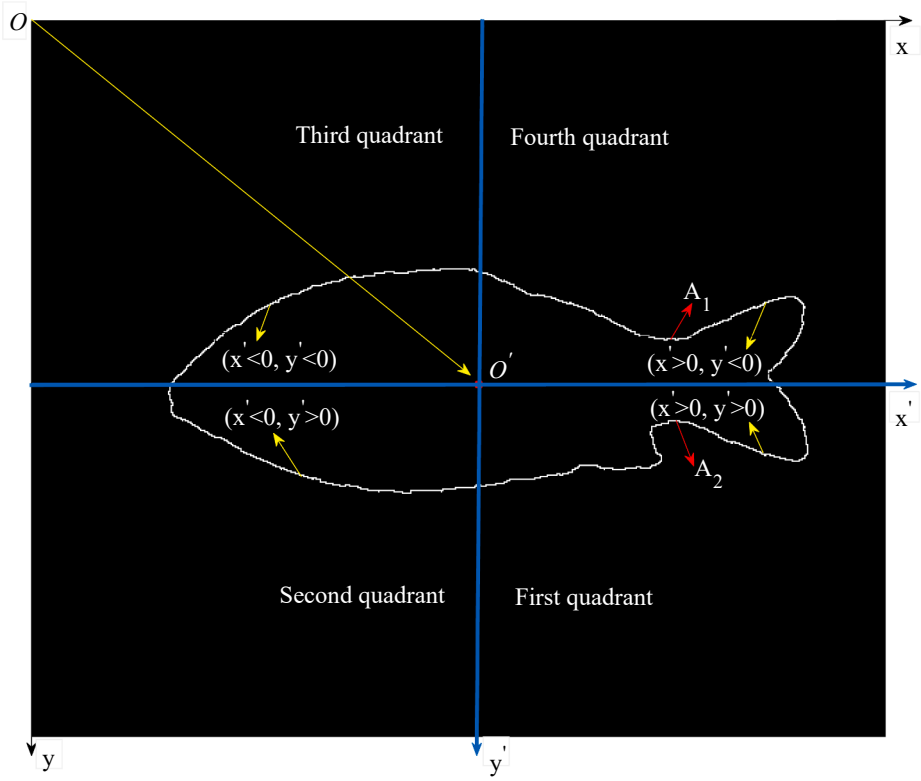

Fig. 3. The fish contour boundary is divided into four regions in the $O^{'}x^{'}y^{'}$ coordinate system.

from the center of image I, that is $0.2*size(I,2) : 0.8*size(I,2)$.

Additionally, the angle between image x-axis and fish binary image F major axis that had the same second moment as the region was calculated as the orientation of fish binary image F. The image was rotated by the orientation of the fish binary image F in order to make binary image major axis orientation parallel to the x-axis of image, which is used for subsequent removal of fish tail fin.

2.3.3. Removal of fish tail fin

When the major axis orientation of fish image is parallel to the x-axis of the image, the fish head must be detected for subsequent caudal fin removal. We proposed an automatic method to detect fish head by the bounding-box, centroid coordinate $D(x_0, y_0)$ and contour pixel coordinate matrix $\boldsymbol{C}_{m\times 2}(x,y)$ of fish binary image. The leftmost and rightmost points of the fish contour can be obtained by the bounding-box. The line that is parallel to the x-axis of the image is passing through centroid coordinate. The distance Z_1 of the leftmost point to the line and the distance Z_2 of the rightmost point to the line were obtained respectively. The difference value between Z_1 and Z_2 determines the direction of the fish's head. When the difference value is less than 0, the fish head is on the left, otherwise it is on the right. The following tail removal process is for the fish head on the left in the image, if the fish head detection is on the right, the image is rotated 180° to make the fish head on the left.

Compared to the other parts of fish body, the tail fin of crucians has a lower specific mass that does not contribute much to the total body mass. Therefore, this paper proposed a fully automatic method to remove fish caudal fin using Cartesian coordinate system and image processing. The main algorithm of removing tail fins can be described step wise as:

***Step.1*. The input image:** The binary image $F_{r\times l}$ of fish.

***Step.2*. Image attribute extraction:** The centroid coordinate $D(x_0, y_0)$ and the contour pixel coordinate $\boldsymbol{C}_{m\times 2}(x,y)$ of binary image F were extracted in Oxy coordinate system.

***Step.3*. Coordinate transformation:** The centroid coordinate $D(x_0, y_0)$ was taken as image origin coordinate $O^{'}$ and the fish contour boundary is divided into four regions in the $O^{'}x^{'}y^{'}$ coordinate system. And the contour pixel coordinates $\boldsymbol{C}^{'}_{m\times 2}(x_i^{'}, y_i^{'})$ is obtained by the difference between contour pixel coordinates $\boldsymbol{C}_{m\times 2}(x_i, y_i)$ and the centroid coordinate $D(x_0, y_0)$, $i = 1\cdots\cdots m$, as shown in Fig. 3.

***Step.4*. Narrow fish tail fin contour range:** In $O^{'}x^{'}y^{'}$ coordinate system, according to fourth quadrant $x_i^{'} > 0, y_i^{'} < 0$, find out all rows i where pixel coordinates $\boldsymbol{C}^{'}_{m\times 2}(x_i^{'}, y_i^{'})$ simultaneously conform to $x_i^{'} \geq 0$, $y_i^{'} \leq 0$, then keep elements in these i rows of $\boldsymbol{C}_{m\times 2}(x_i, y_i)$ unchanged, otherwise, keep these elements in these i rows of $\boldsymbol{C}_{m\times 2}(x_i, y_i)$ become $\boldsymbol{C}_{m\times 2}(0_i, 0_i)$, mark as $\boldsymbol{M}_{m\times 2}(x_i, y_i)$. Similarly, in first quadrant $x_i^{'} > 0$, $y_i^{'} > 0$, find out all rows i where pixel coordinates $\boldsymbol{C}^{'}_{m\times 2}(x_i^{'}, y_i^{'})$ simultaneously conform to $x_i^{'} \geq 0, y_i^{'} \geq 0$, then keep elements in these i rows of $\boldsymbol{C}_{m\times 2}(x_i, y_i)$ unchanged, otherwise, keep these elements in these i rows of $\boldsymbol{C}_{m\times 2}(x_i, y_i)$ become $\boldsymbol{C}_{m\times 2}(0_i, 0_i)$, mark as $\boldsymbol{N}_{m\times 2}(x_i, y_i)$.

***Step.5*. Find the upper point of the tail fin in Oxy coordinate system:** Firstly, find the n_1Â-*th* row where the maximum value of the pixel abscissa from $\boldsymbol{M}_{m\times 2}(x_i, y_i)$. Then, find the n_2Â-*th* row where the maximum value of the pixel ordinate of $\boldsymbol{M}_{m\times 2}(x_i, y_i)$ from first row to n_1Â-*th* row , mark as $A_1 = \boldsymbol{M}(x_{n_2}, y_{n_2})$.

***Step.6*. Find the lower point of the tail fin in Oxy coordinate system:** Firstly, find the n_3Â-*th* row where the maximum value of the pixel abscissa of $\boldsymbol{N}_{m\times 2}(x_i, y_i)$. Find the n_4Â-*th* row where centroid coordinate x_0 of $\boldsymbol{N}_{m\times 2}(x_i, y_i)$. Then, find the row where the minimum value of the pixel ordinate of $\boldsymbol{N}_{m\times 2}(x_i, y_i)$ from n_3Â-*th* row to n_4Â-*th* row, mark the row as $(n_3 + n_5 - 1)$Â-*th* row, and $A_2 = N(x_{n3+n5-1}, y_{n3+n5-1})$.

***Step.7*. Fish tail pixel abscissa positioning and tail fin removal:** The fish tail pixel abscissa $\overline{x} = (x_{n_2} + x_{n3+n5-1})/2$. Set the grayscale value of pixels to be 0 when pixel abscissa is between $\overline{x}$ and l in fish binary image F.

***Step.8*. The output image:** The binary image $F^{'}$ of fish without tail fin. The pseudo code for our proposed fish tail fins removal algorithm is given in Table 2.

Table 2
The pseudo code of the software program for removing the tail fin in automatic mode.

Algorithm of removing tail fin from fish binary image

Input: the binary image $F_{r\times l}$ of fish

Output: the binary image F' of fish without caudal fin

1. The extraction of centroid coordinates $D(x_0, y_0)$ and contour pixel coordinates matrix $C_{m\times 2}$ from **F**
2. $C'(x_i', y_i') \leftarrow C(x_i, y_i) - D(x_0, y_0)$
3. $M_{m\times 2} = N_{m\times 2} = \mathbf{0} \leftarrow$ ***Init***
4. ***for*** $x_i' \geqslant 0$ ***do***
5. ***if*** $y_i' \leqslant 0$ ***then***
6. $M(x_i, y_i) \leftarrow C(x_i, y_i)$
7. ***else***
8. $N(x_i, y_i) \leftarrow C(x_i, y_i)$
9. ***end if***
10. ***end for***
11. $[x_{max1} n_1] \leftarrow \max\{M(:,1)\}$, $[y_{max1} n_2] \leftarrow max\{M(1:n_1, 2)\}, A_1 \leftarrow M(x_{n_2}, y_{n_2})$
12. $[x_{max2} n_3] \leftarrow max\{N(:,1)\}, [x_0 n_4] \leftarrow (N(:,1) == x_0), [y_{min2} n_5] \leftarrow min\ \{N(n_3 : n_4, 2)\}, A_2 \leftarrow N(x_{n_3 + n_5 - 1}, y_{n_3 + n_5 - 1})$
13. $\bar{x} \leftarrow (x_{n_2} + x_{n_3 + n_5 - 1})/2$
14. ***for*** $\bar{x} < j \leq l$ ***do***
15. $F(:, j) = = 0$
16. ***end for***
17. $F' \leftarrow \mathbf{F}$
18. Return $\mathbf{F}'$

2.3.4. Feature extraction and performance estimation

Feature extraction refers to extracting representative information from image to represent the target objects. Generally, the most used features include shape features, texture features and color features. Different types of features are extracted according to research purposes. In order to establish the fish mass estimation model, fish shape features such as length, area, perimeter, volume, width and height are often used to represent image information. In this paper, some features were automatically extracted from fish binary image respectively, including commonly used fish body area (A_1), length (L_1) and height (H_1) from fish with tail fin and body area (A_2), length (L_2) and height (H_2, S_2,T_2) from fish without tail fin.

The Pearson correlation coefficient is used to reflect the degree of linear statistical correlation between two random parameter variables, which is represented by R^2. The greater the R^2 is, the more correlated these two variables are. It is well known that body weight is strongly correlated with morphological characteristics for many animal species. The correlation coefficient can be used as an optimization criterion to evaluate the efficiency of the different measured features to predict fish mass. Therefore, the estimates of Pearson's correlation between feature measurements and body mass were used to compute roughly for the estimation of the relationship between fish features and mass.

2.3.5. Regression algorithm for mass prediction

Multiple linear regression models based on the Partial Least Square (PLS) were evaluated for fish mass prediction. In order to avoid model over-fitting, a 7:3 ratio (i.e. 70% for building mass estimation model and 30% for validating mass prediction) was performed by random stratified sampling. And the dataset from 315 fish was divided into training set containing 220 samples used for fitting models and test set containing 95 samples used for assessing the prediction accuracy of model.

In this paper, to evaluate and compare the models in addition to the coefficient of determination (R^2), the following root mean square error (RMSE), the mean absolute error (MAE) and the maximum relative error (MaxRE) were used in this study as follows.

$$R^2 = \left(1 - \frac{\sum_{i=1}^{N} (y_i' - y_i)^2}{\sum_{i=1}^{N} (y_i' - y_i)^2}\right) \tag{3}$$

$$\mathrm{RMSE} = \sqrt{\frac{\sum_{i=1}^{N} (y_i' - y_i)^2}{N}} \tag{4}$$

$$\mathrm{MAE} = \frac{\sum_{i=1}^{N} (|y_i' - y_i|)}{N} \tag{5}$$

$$\mathrm{MaxRE} = max_{i=1}^{N} \left(\frac{|y_i' - y_i|}{y_i}\right) \tag{6}$$

where y_i' is predicted mass,y_i is the measured mass $\bar{y}_i$ is the mean value of y_i and N is the number of samples. The goodness of fit was qualitatively and quantitatively inspected through a plot depicting the measured mass against the predicted mass.

In addition, standardized regression coefficients are used to compare the effects of different feature variables on mass prediction. The

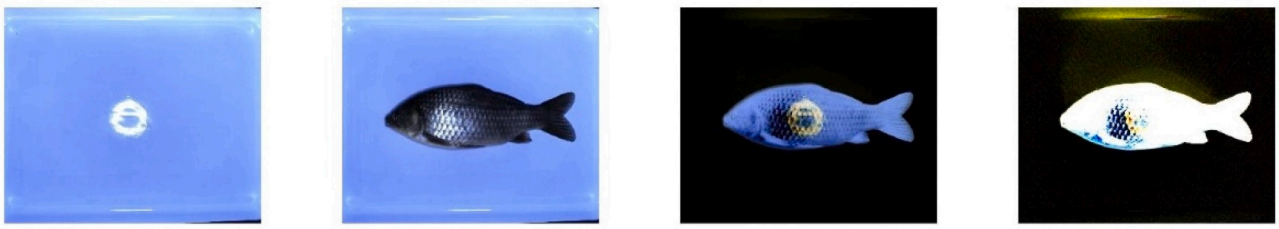

(a) Fixed background image (b) Current fish image (c) Difference image (d) Linear transformation image

Fig. 4. The results of fish image by pre-processing.

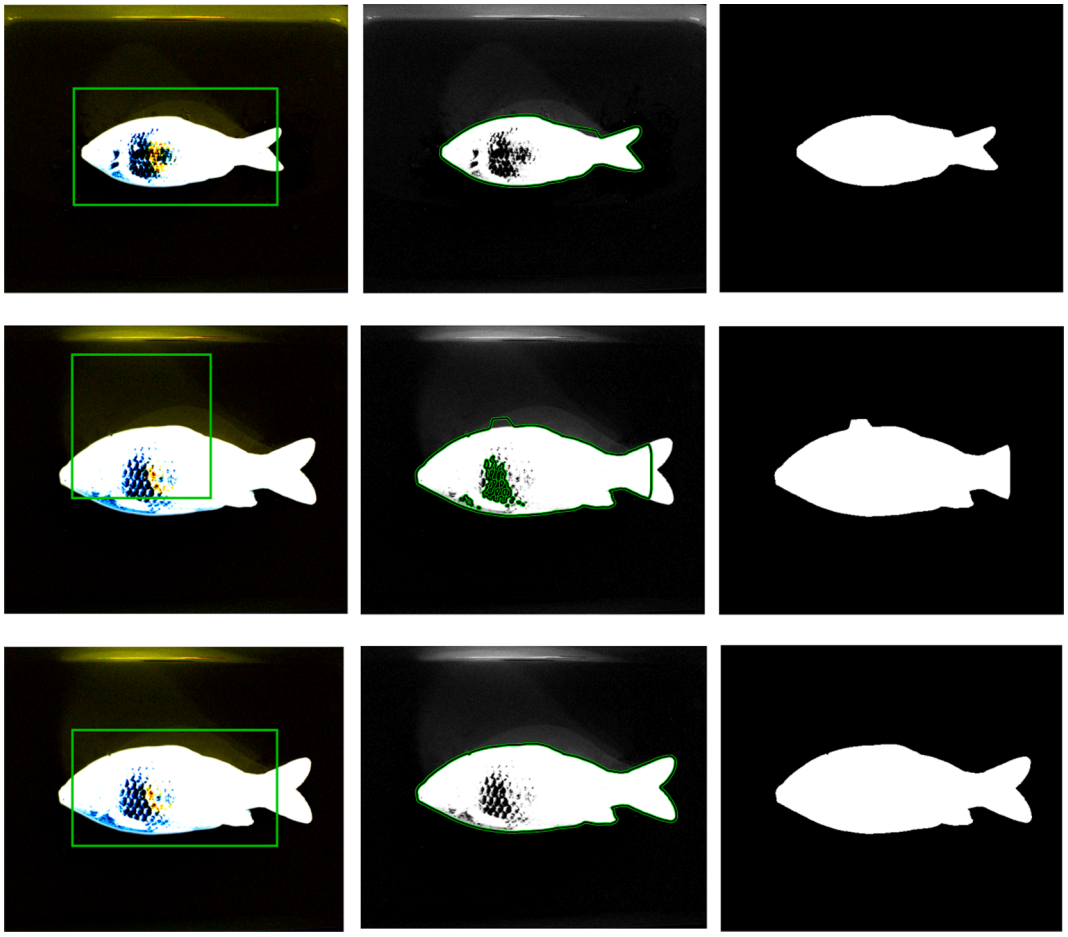

Fig. 5. Comparison of segmentation results. First column: Pre-processing image with initial mask. Second column: Segmentation result using C-V model. Third column: Fish binary image obtained. The first row: C-V model with m(0.3*size(I,1):0.7*size(I,1),0.2*size(I,2):0.8*size(I,2)) and iterative times 400. The second row: C-V model with m(0.1*size(I,1):0.6*size(I,1),0.2*size(I,2):0.6*size(I,2)) and iterative times 500. The third row: using our proposed approach.

standardized regression coefficient is the regression coefficient obtained after standardized processing of independent variable and dependent variable simultaneously. After the standardized data processing, the influence of dimension, order of magnitude and other differences is eliminated so that different variables are comparable, which can be used to compare the effects of different independent variables on dependent variables. The greater the absolute value of the normalized regression coefficient is, the greater its influence on the dependent variable is.

3. Results

3.1. The results of image pre-processing and segmentation

The (a) to (d) in Fig. 4 are the original fish image and the pre-processing fish images. Specifically, the pre-processing fish images include the difference image and linear transformation image. From Fig. 4, it can be seen that the boundaries of the whole fish were clarified by pre-processing, which is useful for later fish image segmentation.

The initial contour contains part of the fish body, which is

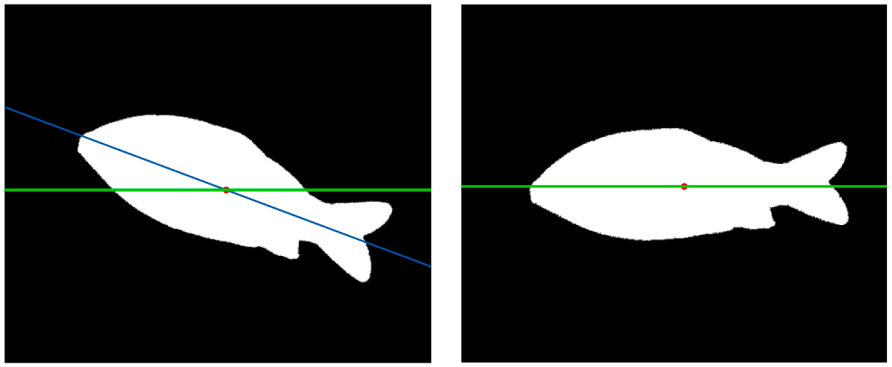

a) The original binary image b) The image after original image was rotated

Fig. 6. Fish image rotated by the orientation between fish major axis and image x-axis.

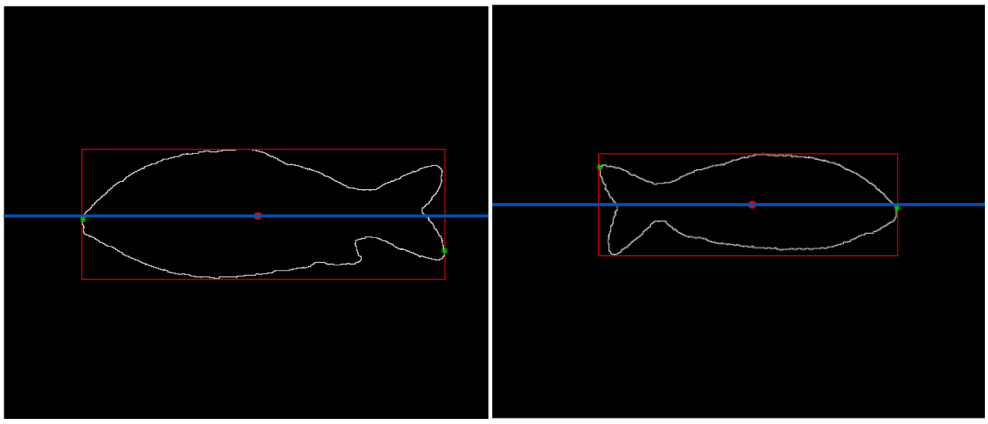

a) The fish head on the left b) The fish head on the right

Fig. 7. The automatic detection of fish head.

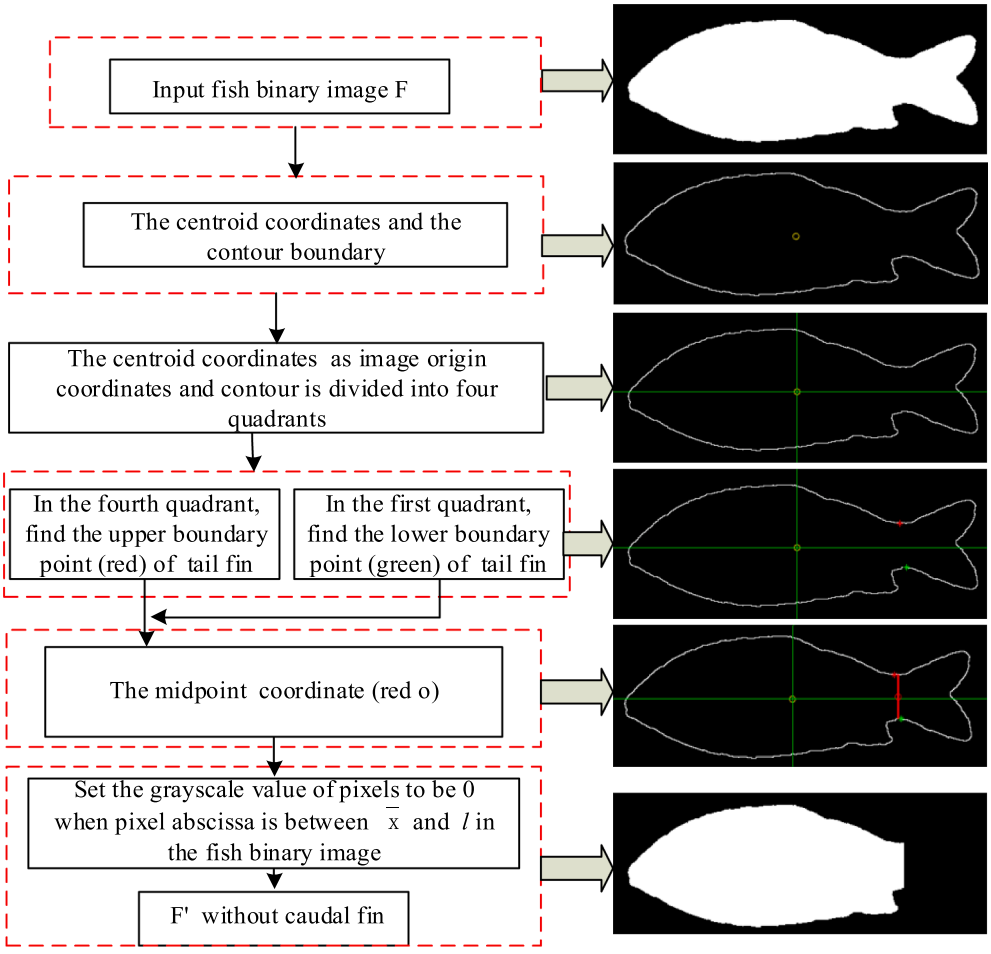

Fig. 8. Flow chart representing the automatic fish tail removal steps operated in MALAB environment on the left. The visual results of some image processing step on the right.

highlighted in green, and the segmentation result is also highlighted in green. Fig. 5 showed the comparison of segmentation results. Our proposed active contour model based on m(0.3*size(I,1):0.7*size (I,1),0.2*size(I,2):0.8*size(I,2)) and iterative times 500 had a good segmentation performance for all images in this study. The wrong position of initial mask and improper iterations result in error segmentation. Hence, the location of initial mask contains as many target objects as possible and appropriate iterative times were selected, which can successfully extract fish boundary.

In addition, in order to make binary image major axis orientation (blue line) parallel to image x-axis (green line), the fish binary image was rotated by the opposite orientation as shown in Fig. 6.

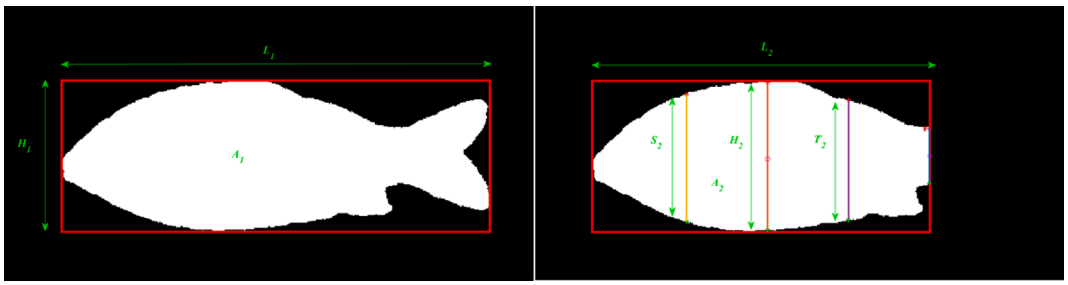

Fig. 9. Features extracted from the fish binary image with and without tail fin.

Table 3
Phenotypic correlations between all measurements (N = 315, *P*-value < 0.001).

	With tail fin			Without tail fin				
	L_1	H_1	A_1	L_2	H_2	A_2	S_2	T_2
L_1	1.000							
H_1	0.916	1.000						
A_1	0.986	0.951	1.000					
L_2				1.000				
H_2				0.952	1.000			
A_2				0.988	0.979	1.000		
S_2				0.958	0.985	0.982	1.000	
T_2				0.954	0.984	0.977	0.977	1.000
Mass	**0.967**	**0.960**	**0.980**	**0.975**	**0.969**	**0.990**	**0.967**	**0.956**

3.2. The results of fish tail fin removal

There are two cases where the fish head is respectively on the left and right, as shown in Fig. 7. The leftmost and rightmost points (green) of the fish contour (white) can be obtained by the bounding box (red). In addition, the line (blue) passing through centroid coordinate (red) is parallel to the x-axis of image. The distance Z_1 of the leftmost point to the line and the distance Z_2 of the rightmost point to the line were obtained respectively. The difference value between Z_1 and Z_2 is less than 0 when the fish head is on the left as shown in Fig. 7 a). Otherwise, the fish head is on the right in Fig. 7 b).

According to the Cartesian coordinate system and image processing, a fully automatic method was proposed to remove fish tail fin without manual intervention. Specifically, by looking for two points above and below caudal fin, the middle point of these two points were defined as the point of the fish tail fin removal. Then, the middle point of the fish tail fin removal was used to remove tail fins from the fish binary image. Fig. 8 shows main procedures and the visual results of fish tail fin removal.

3.3. The results of feature extraction and performance estimation

The relevant description and definition of each feature extracted are given in Table 1. In order to clearly express each feature, these features

Table 4
Comparison of selected models for fish mass prediction (P-value < 0.001).

		Training Dataset				Test Dataset			
Target	Predictors	R2	RMSE(g)	MAE(g)	MaxRE(%)	R2	RMSE(g)	MAE(g)	MaxRE(%)
Mass	H_1	0.952	15.06	11.41	16.0	0.947	15.91	11.49	14.88
	L_1	0.962	13.26	9.32	15.22	**0.958**	**14.26**	**10.22**	**14.62**
	A_1	0.984	8.85	6.69	10.95	0.982	9.47	7.34	11.78
	A_1^2	0.983	9.32	6.61	17.04	0.982	9.63	6.88	16.00
	$A_1^2 + A_1$	**0.986**	**8.47**	**6.06**	**10.64**	**0.985**	**8.94**	**6.51**	**11.64**
	$H_1 + L_1$	0.974	11.29	8.01	12.90	0.972	11.81	8.75	11.52
	$H_1 + A_1$	0.985	8.85	6.69	10.93	0.983	9.47	7.34	10.19
	$L_1 + A_1$	**0.985**	**8.80**	**6.64**	**10.19**	**0.983**	**9.51**	**7.31**	**10.19**
	$L_1 +$ H$_1$, $+$ A$_1$	0.984	8.92	6.74	11.04	0.983	9.54	7.37	10.11
	H_2	0.956	14.50	11.03	13.00	0.956	14.82	11.20	11.98
	L_2	0.969	12.38	9.17	12.72	**0.970**	**12.30**	**9.44**	**10.50**
	A_2	0.989	7.48	5.58	9.42	0.988	8.03	6.00	9.66
	A_2^2	0.990	7.29	5.31	11.06	0.989	7.68	5.75	10.59
	$A_2^2 + A_2$	**0.992**	**6.57**	**4.79**	**8.64**	**0.991**	**7.10**	**5.36**	**8.46**
	$H_2 + L_2$	0.979	10.21	7.67	11.67	0.978	10.52	8.16	9.81
	$H_2 + A_2$	0.989	7.44	5.60	9.27	0.988	8.01	6.09	9.50
	$L_2 + A_2$	**0.989**	**7.44**	**5.57**	**9.03**	**0.988**	**7.95**	**5.94**	**9.48**
	$L_2 + H_2 + A_2$	0.990	7.42	5.60	9.26	0.988	7.98	6.00	9.60

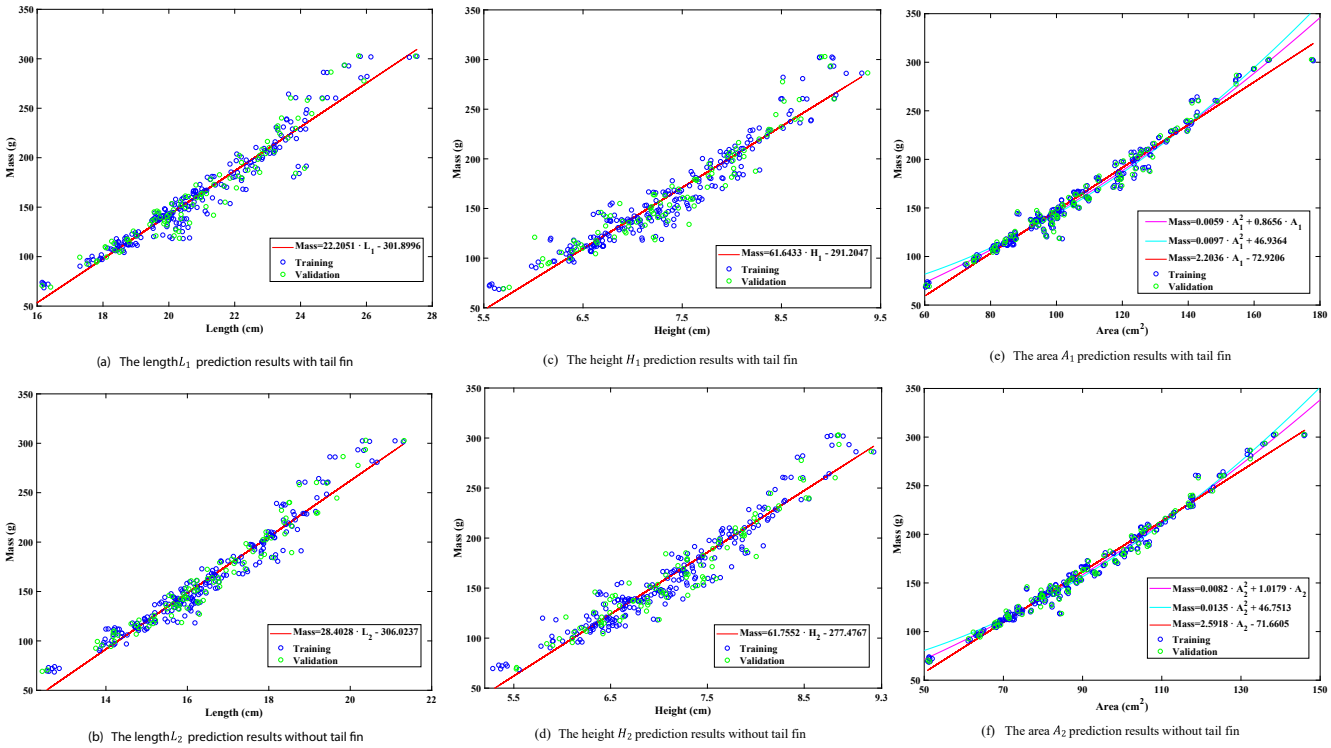

Fig. 10. Visual evaluation of fit goodness for fish mass.

are painted on different parts of fish as shown in Fig. 9. In addition, these feature values were rescaled by using constant dimension of the rectangular reference, which was used to convert all measurements from pixels to cm^2 or mm.

The Pearson correlation coefficient was carried out on fish mass and feature parameters from fish with tail fin and without tail fin. Table 3 shows the estimated Pearson's correlation between shape measurements and fish mass for the datasets. The phenotypic correlations between measured parameters and body mass are positive and high. For fish with tail fin, the R^2 is ranging from 0.960 to 0.980. For the fish without tail fin, the R^2 is ranging from 0.956 to 0.990. The correlation between parameters from fish without tail fin and measured mass was significantly greater than that from fish with tail fin. It can be observed that removing fish tail fin did indeed improve the correlation between shape features and measured mass.

Additionally, the results for phenotypic correlations presented in this study agree with previous results for fish area being the trait that achieved relatively satisfied results (de Verdal et al., 2014; Fernandes et al., 2020; Viazzi et al., 2015). And the parameter with the greatest correlation with the crucian mass was the area A_2 from fish without tail fins with the R^2 of 0.99. The features (S_2, T_2) have a slightly lower correlation with fish mass than other features including L_1, H_1, A_1, L_2,H_2 and A_2. The L_1, H_1, A_1, L_2,H_2 and A_2 were only selected for mass prediction in this study. But these features S_2, T_2 could serve as a reference for future research.

3.4. The results of image derived mass prediction

Table 4 showed the error of mass prediction for fish with and without tail fin in training dataset and test dataset. It was observed that all the models were not significantly different from the manually measured values (P-value < 0.001). Additionally, regarding predictions of fish mass, it was also observed that the model that included only fish area (A_1 or A_2) as predictor variable had better performance on the training dataset or testing dataset than models that included length (L_1 or L_2) or height (H_1 or H_2) predictor variable, as shown in Table 4, which suggest once again that using the fish area is necessary in order to achieve better predicted values. Visual evaluation of fit goodness for fish mass was shown in Fig. 10, including 6 figures of (a)-(f).

From the Table 4, it was also observed that the overall best predictive model included area and its square as predictor variables ($A_1^2 + A_1$ or $A_2^2 + A_2$) and achieved R^2 of 0.985 and 0.991, the RMSE of 8.94 and 7.10, the MAE of 6.51 and 5.36 and the MaxRE of 11.64% and 8.46% for body mass estimation of fish with tail fin and without tail fin, respectively. The precision of mass prediction models can be improved by the removal of fish caudal fin. Scatterplots of measured mass versus predicted mass in test dataset was shown in Fig. 11. It can be seen that the model without caudal fin had relatively better prediction performance than that with caudal fin.

Additionally, the model based on the length (L_1 or L_2) performed better than that based on the height (H_1 or H_2). And the prediction model based on the length L_2 got the better performance with the R^2 of 0.970, the RMSE of 12.30, the MAE of 9.44 and the MaxRE of 10.50% than the mass prediction model that included length L_1 with the R^2 of 0.958, the RMSE of 14.26, the MAE of 10.22 and the MaxRE of 14.62%. It is worth mentioning that the accuracy of the length-mass relationship prediction model without tail fin is better than that with tail fin.

Moreover, Table 4 shows the linear polynomial model based on length, area and height performs a little worse than the model based on length and area as predictor variables. And the coefficients of standardized regression equation based on the three-feature prediction for fish with tail are Zscore (L_1): 0.3183, Zscore (H_1): 0.0460, Zscore (A_1): 0.6321, respectively. The coefficients of standardized regression equation without tail are Zscore (L_2): −0.1607, Zscore (H_2): −0.1236, Zscore (A_2): 1.2684.

4. Discussion

4.1. The removal of fish tail fin

Our proposed method for tail fin removal is different from the method proposed by Viazzi et al. (2015). In Viazzi et al. (2015) study,

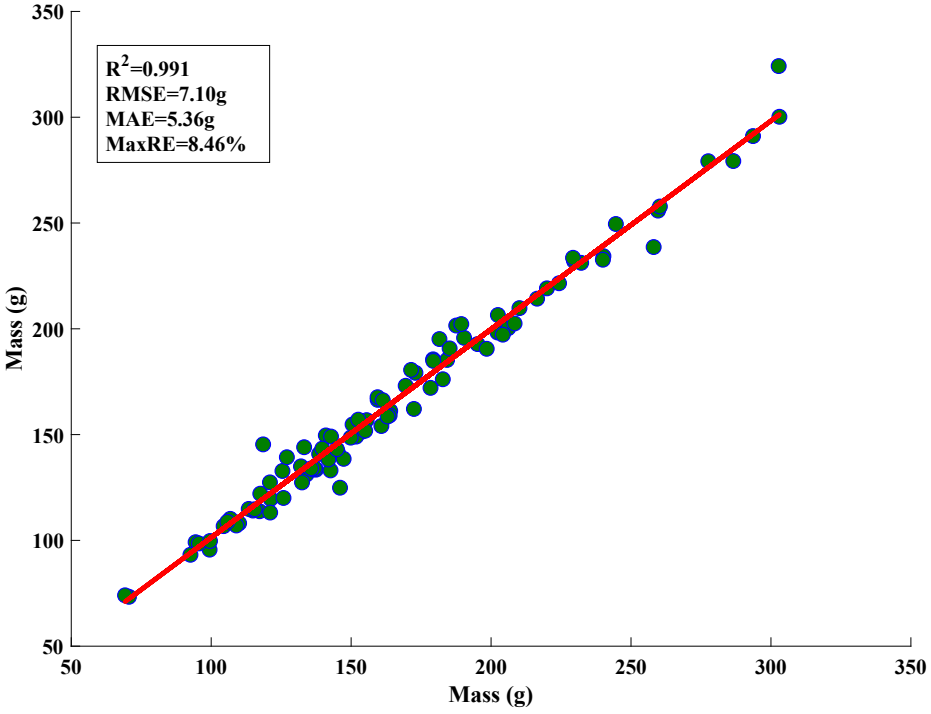

(a) The mass prediction based on fish length and area without tail fin

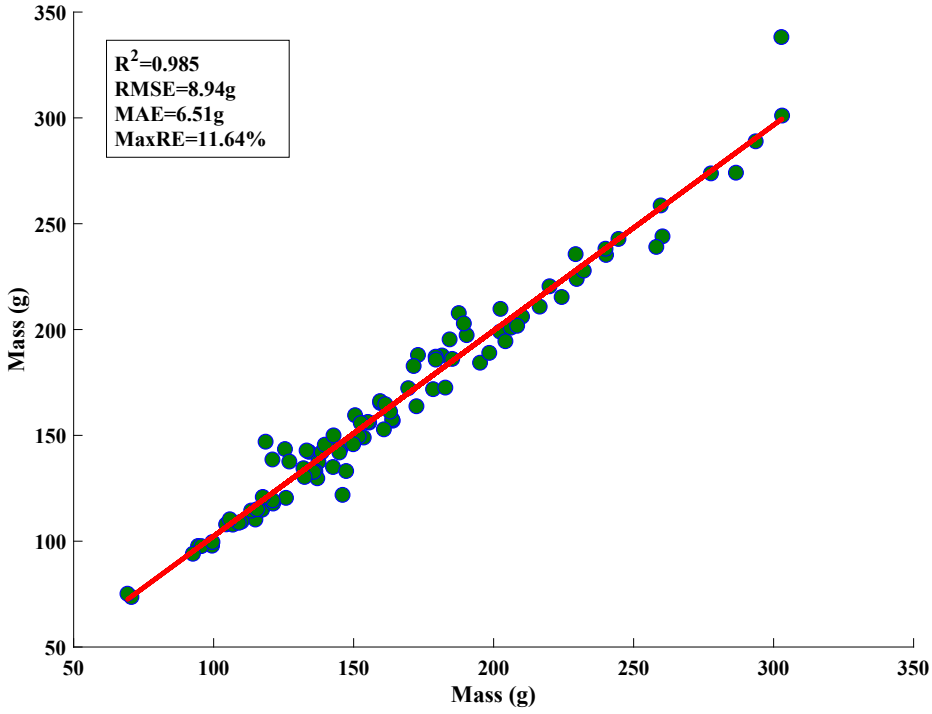

(b) The mass prediction based on fish length and area with tail fin

Fig. 11. Scatterplots of measured mass versus predicted mass in validation set data.

the distance between the pixel of contour and the centroid was calculated to obtain the points of caudal fin that can mark. The points of fish caudal fin were defined by looking at the first and the last peak by human operation. Additionally, these peaks are not obvious for tail fin points, and the removal of tail fin is not perfect. However, our proposed method is to find the midpoint between the two points above and below the caudal fin, and then the midpoint was used to remove the caudal fin completely automatically without human intervention. In addition, Bekkozhayeva et al. (2021) used minimum tail width to remove the tail. However, the 1/4 of the minimum bounding-box rectangle is artificially defined, and the tail fork parts and head direction interfere with finding the position of the vertical line connecting the upper and bottom fish

Table 5
The comparison of different non-supervised methods.

Methods	The theory	Head direction determined	Human intervention	Universality
Viazzi et al. (2015)	The distance between fish contour and centroid coordinate	No	By looking at the first and last peak for the tail points	Jade perch S. barcoo
Bekkozhayeva et al. (2021)	The localization of the point with the minimal height based on last ¼ of the fish body	No	Manually define last ¼ of the fish body	Sumatra barb
Ours	Cartesian coordinate system, fish contour and centroid coordinate	Yes	No	Fish species whose shape of tail fin is similar to that of crucians carp

shape border with the minimal length. The article did not mention how to solve these problems and the detailed implementation steps of this algorithm are not given in this article. Our proposed method can solve the interference of tail fork and the fish head can be automatically detected for completely automatic tail fin removal. These algorithms are also listed in detail in this study. Table 5 shows comparison of different non-supervised methods.

The current popular supervised deep learning can be used to remove fish tail fin. However, a large number of training samples are required to be manually marked and different person markers could introduce errors. Since the removal of tail fins is time-consuming and laborious, there are no effective non-supervised methods for fish caudal fin removal in available literatures. As far as we know, the proposed non-supervised method is the original design to remove fully automatically fish tail fin, which not only could improve accuracy of mass prediction but also will help achieve full automation of aquaculture. In addition, the mass prediction model based on features extracted from fish without tail fin could be used to further accurately predict biomass of free-swimming fish underwater. Therefore, the removal of fish tail fin is highly necessary for establishing relationship model between mass and features without tail fin. And other fins will be considered to remove from fish by other methods in future studies.

Meanwhile, the proposed methodology of tail fin removal can be applied to other fish species whose shape of tail fin is similar to that of crucians carp. Although this method is not applicable to all species of fish, the proposed non-supervised method can provide a reference for caudal fin removal. Future directions on the development of other fish fin removal should also consider with other methodology such as curvature, which can more accurately predict the biomass of free-swimming fish underwater.

4.2. Image derived mass prediction

In order to further demonstrate the superiority of tail fin removal, we compare the accuracy of models between fish mass and extracted features with tail fin and without tail fin. From Table 4, it becomes evident that the results of all models were better when the tail fin is removed from fish image, which was furthermore confirmed that removing the tail fin can improve the mass prediction model precision. The model that included fish area, length and height as predictor variables performs slightly worse than the model based on area and length as predictor variables. The coefficients of the standardized regression equation are Zscore (A_1):0.6321 > Zscore (L_1): 0.3183 > Zscore (H_1): 0.0460 and Zscore (A_2): 1.2684 > Zscore (L_2): 0.1607 > Zscore (H_2): 0.1236, which indicated area factor has highest contribution to the mass prediction and then it is the length factor whether the fish tail is removed or not. The height factor has a little contribution to mass prediction. In addition, the model based on area and its square as predictor variables without tail fins achieved the highest predictions for fish mass on the training dataset and test dataset. The reason may be that different parts of fish have different mass density. The area vary greatly whether the tail is removed or not and the overall mass density is relatively uniform when tail is removed, therefore using the on area and its square as parameters has the best performance. These findings have important guiding significance to select which characteristics to estimate fish mass in future research.

In addition, compared with the linear model based on length or height, the linear model that included the area of fish with and without caudal fin for mass prediction had a better performance with the R^2 of 0.982, 0.988, the RMSE of 9.47, 8.03, the MAE of 7.34, 6.00 and the MaxRE of 11.78%, 9.66%, respectively, which has worse performance than the model based on area and its square as predictor variables. Compared with the mass prediction model based on other features, the model based on area and area square perform best to predict the mass in test dataset as shown in Table 4. However, this study about the model based on area and its square to predict mass of free-swimming fish has not been found in existing literatures. The caudal fin of free-swimming fish underwater is always deformed or bent, which causes errors in size measurement using computer vision, further resulting in errors for mass measurement. Moreover, the established model based on area and its square without tail fins is more accurate to predict fish mass. Therefore, the developed mathematical model included area and area square as predictor variables extracted from fish without tail fin is necessary to be applied for mass estimation of free-swimming fish underwater. In future works, this established mass prediction model based on area and area square as predictor variables can be used to estimate mass of free-swimming fish in water with binocular camera, which provides a reference for mass estimation of free-swimming fish in future.

5. Conclusion

This paper proposed a fully automatic method of tail fin removal based on Cartesian coordinate system and image analysis, which is of great significance for meeting the precision and level of intelligence in intensive aquaculture. The features respectively extracted from fish images with and without tail fin were used to develop fish mass prediction model by the PLS. The experimental results showed that this proposed method of caudal fin removal is very helpful for more accurate estimation of fish mass. In addition, the model with fish area and its square area as variables extracted from fish without considering tail fin showed a better performance in test dataset ($R^2 = 0.991$, RMSE = 7.10 g, MAE = 5.36 g, MaxRE = 8.46%). The performance of the model based on area and area square can be improved by removing the tail fin, which illustrated automatic tail fin removal is very necessary to accurately estimate the mass of crucians from fish image. Finally, the mass prediction model based on area and length extracted from fish without tail fin perform best, which could be used to further predict biomass of free-swimming fish underwater more accurately in future research.

CRediT authorship contribution statement

Yinfeng Hao: Conceptualization, Methodology, Software, Validation, Investigation, Data curation, Writing – original draft, Visualization, Writing – review & editing. **Hongjian Yin:** Resources, Project administration. **Daoliang Li:** Conceptualization, Supervision, Funding acquisition.

Declaration of Competing Interest

The authors declare that they have no known competing financial interests or personal relationships that could have appeared to influence the work reported in this paper.

Acknowledgement

This work was supported by the National Natural Science Fundation of China (Grant No.62076244) "Study on characteristics recognition and behavior analysis of swimming fish feeding population based on machine vision''. The authors would also like to thank the professional expert for proofreading this article.

References

Al-Jubouri, Q., Al-Nuaimy, W., Al-Taee, M., Young, I., 2017. An automated vision system for measurement of zebrafish length using low-cost orthogonal web cameras. Aquac. Eng. 78, 155–162. https://doi.org/10.1016/j.aquaeng.2017.07.003.

Ashley, P.J., 2007. Fish welfare: current issues in aquaculture. Appl. Anim. Behav. Sci. 104 (3-4), 199–235. https://doi.org/10.1016/j.applanim.2006.09.001.

Atienza-Vanacloig, V., Andreu-Garcia, G., Lopez-Garcia, F., Valiente-Gonzalez, J.M., Puig-Pons, V., 2016. Vision-based discrimination of tuna individuals in grow-out cages through a fish bending model. Comput. Electron. Agric. 130, 142–150. https://doi.org/10.1016/j.compag.2016.10.009.

Balaban, M.O., Chombeau, M., Cirban, D., Gumus, B., 2010a. Prediction of the Weight of Alaskan Pollock Using Image Analysis. J. Food Sci. 75, E552–E556. https://doi.org/10.1111/j.1750-3841.2010.01813.x.

Balaban, M.O., Sengor, G.F.U., Gil Soriano, M., Guillen Ruiz, E., 2010b. Using Image Analysis to Predict the Weight of Alaskan Salmon of Different Species. J. Food Sci. 75, E157–E162. https://doi.org/10.1111/j.1750-3841.2010.01522.x.

Beddow, T.A., Ross, L.G., Marchant, J.A., 1996. Predicting salmon biomass remotely using a digital stereo-imaging technique. Aquaculture 146 (3-4), 189–203.

Bekkozhayeva, D., Saberioon, M., Cisar, P., 2021. Automatic individual non-invasive photo-identification of fish (Sumatra barb Puntigrus tetrazona) using visible patterns on a body. Aquac. Int. 29 (4), 1481–1493. https://doi.org/10.1007/s10499-021-00684-8.

Chan, T.F., Vese, L.A., 2001. Active contours without edges. ITIP 10, 266-277. https://doi.org/10.1109/83.902291.

Costa, C., Antonucci, F., Boglione, C., Menesatti, P., Vandeputte, M., Chatain, B., 2013. Automated sorting for size, sex and skeletal anomalies of cultured seabass using external shape analysis. Aquac. Eng. 52, 58–64. https://doi.org/10.1016/j.aquaeng.2012.09.001.

Costa, C., Scardi, M., Vitalini, V., Cataudella, S., 2009. A dual camera system for counting and sizing Northern Bluefin Tuna (Thunnus thynnus; Linnaeus, 1758) stock, during transfer to aquaculture cages, with a semi automatic Artificial Neural Network tool. Aquaculture 291, 161–167. https://doi.org/10.1016/j.aquaculture.2009.02.013.

de Verdal, H., Vandeputte, M., Pepey, E., Vidal, M.-O., Chatain, B., 2014. Individual growth monitoring of European sea bass larvae by image analysis and microsatellite genotyping. Aquaculture 434, 470–475. https://doi.org/10.1016/j.aquaculture.2014.09.012.

Dios, J., Serna, C., Ellero, A., 2003. Computer vision and robotics techniques in fish farms. Robotica 21, 233–243. https://doi.org/10.1017/s0263574702004733.

FAO, 2020. The state of food security and nutrition in the world 2020. https://doi.org/http://www.fao.org/3/ca9692en/CA9692EN.pdf.

Fernandes, A.F.A., Turra, E.M., de Alvarenga, E.R., Passafaro, T.L., Lopes, F.B., Alves, G. F.O., Singh, V., Rosa, G.J.M., 2020. Deep Learning image segmentation for extraction of fish body measurements and prediction of body weight and carcass traits in Nile tilapia. Comput. Electron. Agric. 170 https://doi.org/10.1016/j.compag.2020.105274.

Garcia, R., Prados, R., Quintana, J., Tempelaar, A., Gracias, N., Rosen, S., Vagstol, H., Lovall, K., 2020. Automatic segmentation of fish using deep learning with application to fish size measurement. ICES J. Mar. Sci. 77, 1354–1366. https://doi.org/10.1093/icesjms/fsz186.

Gonzalez, R.C., Woods, R,E., Eddins, S,L., 2018. Digital Image Processing Using MATLAB [M]. Second Edition.

Kass, M., Witkin, A., Terzopoulos, D., 1987. SNAKES - ACTIVE CONTOUR MODELS. Int J Comput Vision 1, 321–331. https://doi.org/10.1007/bf00133570.

Klontz, G.W., Kaiser, H., 1993. Producing a marketable fish. Focus on renewable natural resources (USA). https://doi.org/europepmc.org/article/AGR/IND20392509.

Konovalov, D.A., Saleh, A., Efremova, D.B., Domingos, J.A., Jerry, D.R., Ieee, 2019. Automatic Weight Estimation of Harvested Fish from Images. J Syst Sci Syst Eng, 308-314. https://doi.org/10.1109/DICTA47822.2019.8945971.

Li, D., Hao, Y., Duan, Y., 2020. Nonintrusive methods for biomass estimation in aquaculture with emphasis on fish: a review. Rev. Aquac. 12, 1390–1411. https://doi.org/10.1111/raq.12388.

Lines, J.A., Tillett, R.D., Ross, L.G., Chan, D., Hockaday, S., McFarlane, N.J.B., 2001. An automatic image-based system for estimating the mass of free-swimming fish. Comput. Electron. Agric. 31, 151–168. https://doi.org/10.1016/s0168-1699(00)00181-2.

Manuel Miranda, J., Romero, M., 2017. A prototype to measure rainbow trout's length using image processing. Aquac. Eng. 76, 41–49. https://doi.org/10.1016/j.aquaeng.2017.01.003.

Monkman, G.G., Hyder, K., Kaiser, M.J., Vidal, F.P., 2020. Accurate estimation of fish length in single camera photogrammetry with a fiducial marker. ICES J. Mar. Sci. 77, 2245–2254. https://doi.org/10.1093/icesjms/fsz030.

Munoz-Benavent, P., Andreu-Garcia, G., Valiente-Gonzalez, J.M., Atienza-Vanacloig, V., Puig-Pons, V., Espinosa, V., 2018a. Automatic Bluefin Tuna sizing using a stereoscopic vision system. ICES J. Mar. Sci. 75, 390–401. https://doi.org/10.1093/icesjms/fsx151.

Munoz-Benavent, P., Andreu-Garcia, G., Valiente-Gonzalez, J.M., Atienza-Vanacloig, V., Puig-Pons, V., Espinosa, V., 2018b. Enhanced fish bending model for automatic tuna sizing using computer vision. Comput. Electron. Agric. 150, 52–61. https://doi.org/10.1016/j.compag.2018.04.005.

Odone, F., Trucco, E., Verri, A., 2001. A trainable system for grading fish from images. Appl. Artif. Intell. 15, 735–745. https://doi.org/10.1080/08839510317018573.

Puig-Pons, V., Munoz-Benavent, P., Espinosa, V., Andreu-Garcia, G., Valiente-Gonzalez, J.M., Estrucha, V.D., Ordonez, P., Perez-Arjona, I., Atienza, V., Melich, B., de la Gandara, F., Santaella, E., 2019. Automatic Bluefin Tuna (Thunnus thynnus) biomass estimation during transfers using acoustic and computer vision techniques. Aquac. Eng. 85, 22–31. https://doi.org/10.1016/j.aquaeng.2019.01.005.

Rizzo, A.A., Welsh, S.A., Thompson, P.A., 2017. A paired-laser photogrammetric method for in situ length measurement of benthic fishes. N. Am. J. Fish. Manag. 37, 16–22. https://doi.org/10.1080/02755947.2016.1235632.

Saberioon, M., Cisar, P., 2018. Automated within tank fish mass estimation using infrared reflection system. Comput. Electron. Agric. 150, 484–492. https://doi.org/10.1016/j.compag.2018.05.025.

Saberioon, M., Gholizadeh, A., Cisar, P., Pautsina, A., Urban, J., 2017. Application of machine vision systems in aquaculture with emphasis on fish: state-of-the-art and key issues. Rev. Aquac. 9, 369–387. https://doi.org/10.1111/raq.12143.

Shi, C., Wang, Q., He, X., Zhang, X., Li, D., 2020. An automatic method of fish length estimation using underwater stereo system based on LabVIEW. Comput. Electron. Agric. 173 https://doi.org/10.1016/j.compag.2020.105419.

Siewert, C., Daenicke, S., Kersten, S., Brosig, B., Rohweder, D., Beyerbach, M., Seifert, H., 2014. Difference method for analysing infrared images in pigs with elevated body temperatures. Z. Med. Phys. 24, 6–15. https://doi.org/10.1016/j.zemedi.2013.11.001.

Viazzi, S., Van Hoestenberghe, S., Goddeeris, B.M., Berckmans, D., 2015. Automatic mass estimation of Jade perch Scortum barcoo by computer vision. Aquac. Eng. 64, 42–48. https://doi.org/10.1016/j.aquaeng.2014.11.003.

Zhang, L., Wang, J., Duan, Q., 2020. Estimation for fish mass using image analysis and neural network. Comput. Electron. Agric. 173 https://doi.org/10.1016/j.compag.2020.105439.

Zhou, C., Lin, K., Xu, D., Chen, L., Guo, Q., Sun, C., Yang, X., 2018. Near infrared computer vision and neuro-fuzzy model-based feeding decision system for fish in aquaculture. Comput. Electron. Agric. 146, 114–124. https://doi.org/10.1016/j.compag.2018.02.006.

Zhou, C., Lin, K., Xu, D., Liu, J., Zhang, S., Sun, C., Yang, X., 2019a. Method for segmentation of overlapping fish images in aquaculture. Int. J. Agr. Biol. Eng. 12, 135–142. https://doi.org/10.25165/j.ijabe.20191206.3217.

Zhou, C., Xu, D., Chen, L., Zhang, S., Sun, C., Yang, X., Wang, Y., 2019b. Evaluation of fish feeding intensity in aquaculture using a convolutional neural network and machine vision. Aquaculture 507, 457–465. https://doi.org/10.1016/j.aquaculture.2019.04.056.

Zion, B., 2012. The use of computer vision technologies in aquaculture - a review. Comput. Electron. Agric. 88, 125–132. https://doi.org/10.1016/j.compag.2012.07.010.